

Random Wins All: Rethinking Grouping Strategies for Vision Tokens

Qihang Fan^{1,2}, Yuang Ai^{1,2}, Huaibo Huang^{1*}, Ran He^{1,2}

¹MAIS & NLPR, Institute of Automation, Chinese Academy of Sciences, Beijing, China

²School of Artificial Intelligence, University of Chinese Academy of Sciences, Beijing, China

fanqihang.159@gmail.com, shallowdream555@gmail.com,

huaibo.huang@cripac.ia.ac.cn, rhe@nlpr.ia.ac.cn

Abstract

Since Transformers are introduced into vision architectures, their quadratic complexity has always been a significant issue that many research efforts aim to address. A representative approach involves grouping tokens, performing self-attention calculations within each group, or pooling the tokens within each group into a single token. To this end, various carefully designed grouping strategies have been proposed to enhance the performance of Vision Transformers. Here, we pose the following questions: **Are these carefully designed grouping methods truly necessary? Is there a simpler and more unified token grouping method that can replace these diverse methods?** Therefore, we propose the random grouping strategy, which involves a simple and fast random grouping strategy for vision tokens. We validate this approach on multiple baselines, and experiments show that random grouping almost outperforms all other grouping methods. For example, compared to the classic Swin Transformer, our random grouping strategy achieves improvements of **+1.3**, **+0.9**, and **+0.9** across three model sizes. When transferred to downstream tasks, such as object detection, random grouping demonstrates even more pronounced advantages. In response to this phenomenon, we conduct a detailed analysis of the advantages of random grouping from multiple perspectives and identify several crucial elements for the design of grouping strategies: **positional information, head feature diversity, global receptive field, and fixed grouping pattern**. We demonstrate that as long as these four conditions are met, vision tokens require only an extremely simple grouping strategy to efficiently and effectively handle various visual tasks. We also validate the effectiveness of our proposed random method across multiple modalities, including visual tasks, point cloud processing, and vision-language models. Code will be available at <https://github.com/qhfan/random>.

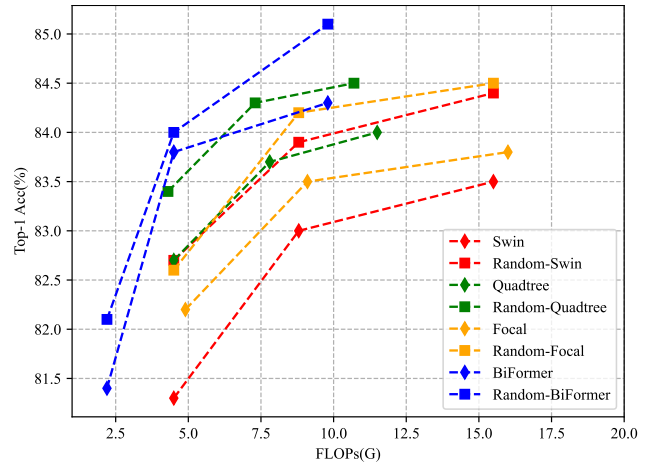


Figure 1. Comparison among baselines and our methods. Random Grouping strategy outperforms all baselines.

1. Introduction

Transformer, as a powerful architecture, is first introduced in the field of NLP and subsequently finds extensive applications in computer vision [9, 35]. It achieves remarkable success in various vision tasks such as image classification, object detection, instance segmentation, and semantic segmentation.

However, Transformer faces a significant issue: its core operator, self-attention, has quadratic complexity. As the number of vision tokens increases, the computational load of the Vision Transformer grows substantially, greatly limiting its applicability. In recent years, many works attempt to address this issue. Among these efforts, a highly representative approach involves grouping vision tokens. After grouping, self-attention calculations are performed within each group [8, 11, 24, 38, 50], or tokens within the same group are fused into a single token, followed by global attention calculations [14, 36, 37, 41]. Specifically, Swin Transformer [24] divides all tokens into non-overlapping windows, with self-attention calculations performed within each window. Quadtree [32], on the other hand, adopts a context-aware grouping method, using a tree structure to

*Huaibo Huang is the corresponding author.

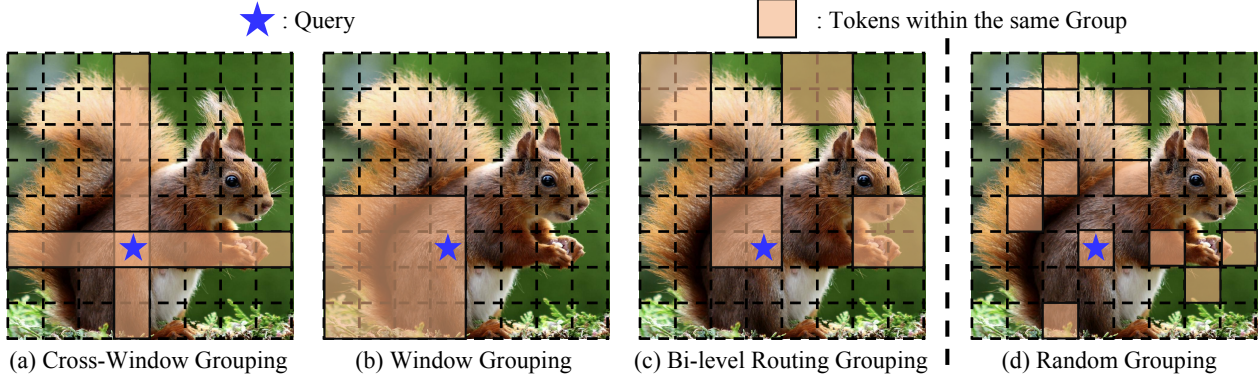


Figure 2. Comparison among different token grouping strategies.

hierarchically group tokens from coarse to fine granularity. BiFormer [50] strikes a balance between the two, combining the context-aware grouping characteristic of Quadtree with the efficiency of grouping seen in Swin Transformer. CrossFormer [38] not only uses a window-based grouping method but also employs a dilated grouping approach, enabling the model to simultaneously perceive both local and global features.

However, although many carefully designed grouping methods enhance model performance, the complex operations involved in the grouping process significantly impact efficiency and make deployment challenging. This raises the question: are these intricate, meticulously designed grouping methods truly necessary? Is there a simpler and more unified grouping method that can replace these approaches?

Based on this consideration, we propose an extremely simple token grouping strategy: random grouping strategy, as illustrated in Fig. 2. Unlike many methods that require complex grouping operations [13, 32, 45, 50], random grouping simply divides all vision tokens into equal segments randomly. Self-attention or pooling is then performed within each group. This random grouping method is not only applicable to basic image classification tasks but also easily transferable to downstream tasks such as object detection and semantic segmentation. Besides, the random group strategy also can be applied to 3D vision tasks such as point cloud segmentation. We experiment with this extremely simple random grouping strategy on various baselines and are surprised to find that this straightforward random approach easily outperforms most of the baselines. Specifically, as shown in Fig. 1, Random-Swin, which employs the random grouping strategy, improves by **+1.3**, **+0.9**, and **+0.9** across different model scales compared to the baseline Swin Transformer. This improvement is even more pronounced in downstream tasks such as object detection. Beyond the visual tasks, the random pattern also can be applied to point cloud task and vision-language models.

In response to this phenomenon, we explain from multiple angles why random grouping achieves such remark-

able results. We demonstrate that as long as the four conditions—**positional information**, **head feature diversity**, **global receptive field**, and a **fixed grouping pattern**—are met, even very simple random grouping methods enable visual models to achieve good results.

Our contributions can be summarized as follows:

- We propose a random grouping strategy, an extremely simple and fast grouping method, to reduce the complexity and computational load of Vision Transformers.
- We conduct extensive experiments on various baselines and find that this simple strategy not only offers fast inference speed but also outperforms most carefully designed vision token grouping methods.
- We analyze the reasons behind the excellent performance of random grouping and identify four key factors that impact the performance of random grouping. We find that as long as these four elements are satisfied, even a simple grouping method can achieve outstanding performance.

2. Related Works

Vision Transformers. Transformers originate in the field of NLP and are later introduced to various tasks in computer vision [9, 35]. The superior performance of Vision Transformers has garnered significant attention. Many works propose improvements to Vision Transformers; some aim to enhance data efficiency, while others focus on improving computational efficiency [7, 10, 12, 20, 23, 26, 29, 31, 34, 39, 44, 46]. Specifically, DeiT [33] incorporates extensive data augmentation [4, 28, 49] into the training process of Vision Transformers and improves data efficiency through model distillation. EViT [20] enhances the computational efficiency of Vision Transformers by reducing the number of tokens through the fusion of less important tokens. Aside from these methods, one class of approaches, represented by Swin Transformer [24], groups vision tokens based on spatial features or clustering results and performs self-attention calculations within each group. Another class of approaches, represented by PVT [36], merges vision tokens within the same group into a single token before performing global attention calculations.

Grouping Strategies for Vision Tokens. As an important approach to addressing the quadratic complexity of Vision Transformers, grouping vision tokens is integral to many Vision Transformer designs. For example, the classic Swin-Transformer [24] directly groups vision tokens into windows, which limits the receptive field of each token and thereby reduces the complexity of computing self-attention. CSwin-Transformer [8] groups tokens into a cross-window shape, aiming to maximize the receptive field of each token. In addition to these relatively simple and fast methods, there are approaches that use more complex operations for token grouping. For instance, Quadtree [32] employs a tree structure to hierarchically group tokens, while BiFormer [50] uses a bi-level routing method for token grouping. From the simplest method of partitioning tokens based on their spatial positions [7, 8, 14, 15, 24, 27, 37] to more sophisticated approaches that group tokens according to their semantic information [11, 23, 32, 41, 50], model performance improves progressively, but the design of token grouping becomes increasingly complex. To this end, we aim to propose a simple and unified grouping strategy to replace the diverse methods currently in use. Additionally, we seek to identify the key factors that truly contribute to the effectiveness of grouping strategies.

3. Method

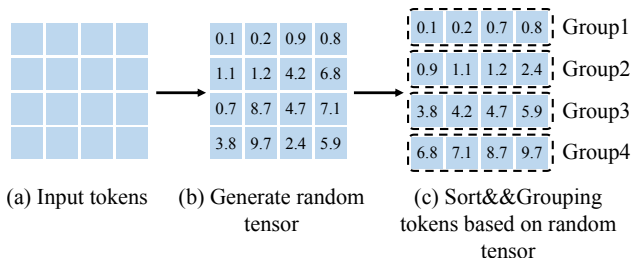


Figure 3. Illustration of the random grouping strategy.

In this section, we explain our proposed random grouping strategy. For simplicity, the subsequent description focuses solely on the single-head scenario.

Generate Random Tensor. For the input tokens $X \in \mathbb{R}^{h \times w \times d}$, we first generate a random tensor $P \in \mathbb{R}^{h \times w}$ based on the resolution of X . The shape of tensor P in the height and width dimensions are the same as those of the input X . This means that P corresponds to X on a one-to-one basis, as illustrated in Fig. 3. **Once the tensor P is generated, it is stored. Then, the input tokens of each subsequent image will correspond one-to-one with this stored P .**

Sort Random Tensor. After obtaining P , we sort P in descending order. Since P corresponds to X on a one-to-one basis, X is also sorted in the same order as P . **It is**

worth noting that because P is fixed after it is generated, the input tokens for each image are arranged in the same order.

Group Vision Tokens. We denote the rearranged X based on P as X_p . By sequentially dividing X_p into equal parts, we obtain the grouped tokens. Since X_p is already randomly shuffled, simply dividing X_p equally will yield the randomly grouped tokens.

Apply P to Higher Resolutions. Since P is fixed once it is generated and its shape is fixed at $h \times w$, it cannot be directly applied to higher resolution tasks such as object detection, instance segmentation, and semantic segmentation. Therefore, when applying P to higher resolution scenarios, we use nearest-neighbor interpolation to adjust P to match the shape of the input tokens.

Multi-Head Setting. The above discussion focuses on the single-head scenario. To easily extend this to the multi-head case, we change the shape of the randomly generated tensor P from $h \times w$ to $n \times h \times w$, where n is the number of heads. This means that we use different random tensors to sort the tokens for each head, which results in different random grouping outcomes for each head.

Simplicity and Efficiency. We did not spend much time describing the random grouping strategy, as it is exceedingly simple. Nevertheless, it outperforms the vast majority of complex grouping methods across many visual tasks, including image classification, object detection, instance segmentation, semantic segmentation, and point cloud segmentation. Additionally, due to its simplicity, it achieves various degrees of acceleration compared to baseline methods. However, the fact that such a seemingly arbitrary method yields excellent results is counterintuitive. Consequently, we dedicate substantial discussion in subsequent sections to attempt to explain this phenomenon.

Baselines. We categorize the baselines into three types: **plain backbones**, **partition-based backbones** that group tokens and perform self-attention within each group, and **pooling-based backbones** that group tokens and pool them into a single token for further processing. For plain backbones, we apply random grouping and perform self-attention within each group. For the remaining two types, we simply replace their token grouping methods with random grouping.

4. Experiments

To validate the superiority of the random grouping strategy over other methods, we conduct extensive experiments

based on multiple baselines, including image classification, object detection, instance segmentation, and semantic segmentation. We also conducted point cloud segmentation based on the point transformer v3 [40]. Besides, we apply random pattern to LLaVA-1.5 [22] to evaluate the random pattern’s effectiveness on vision language model.

4.1. Image Classification

Settings. We train our models on ImageNet-1K [6] from scratch. We follow the same training strategy in the baselines[24, 33, 36], with the only supervision being classification loss for a fair comparison. We use the AdamW optimizer with a cosine decay learning rate scheduler to train the models, and set the initial learning rate, weight decay, and batch size to 0.001, 0.05, and 1024, respectively. We adopt the strong data augmentation and regularization used in baselines [8, 24, 33, 50], such as RandAugment [4] (randm9-mstd0.5-inc1), Mixup [48] (prob=0.8), CutMix [47] (prob=1.0), and Random Erasing [49] (prob=0.25).

Results. We show the classification results in the Tab. 1. It is evident that compared to the grouping strategies used in other methods, the random grouping strategy demonstrates clear advantages in both speed and performance. Specifically, on the plain backbone, the random grouping strategy reduces the computational load of DeiT, effectively enhancing its speed and performance. Compared to the various grouping strategies in partition-based models, the random grouping strategy also demonstrates better performance and superior inference speed. Specifically, compared to the strategy used in Quadtree, the random grouping strategy achieves more than a threefold increase in speed and a significant performance improvement. Similar conclusions can be drawn when comparing with pooling-based backbones.

4.2. Object Detection and Instance Segmentation

Settings. Following baselines, we adopt MMDetection [1] to implement RetinaNet [21] and Mask-RCNN [17] to validate the effect of random grouping on object detection and instance segmentation. We use the commonly used “1×” (12 training epochs) setting for the RetinaNet and Mask R-CNN. Following baselines [24, 37, 50], during training, images are resized to the shorter side of 800 pixels while the longer side is within 1333 pixels. We adopt the AdamW optimizer with a learning rate of 0.0001 and batch size of 16 to optimize the model. The learning rate declines with the decay rate of 0.1 at the epoch 8 and 11.

Results. We show the comparison results in the Tab. 2. From these results, it is evident that our proposed random grouping strategy achieves improvements in both object detection and instance segmentation, whether using a partition-based backbone or a pooling-based back-

Model	Params FLOPs Throughput [↑]			Acc (%)
	(M)	(G)	(imgs/s)	
Plain Backbone				
DeiT-T [33]	6	1.3	6433	72.2
Random-DeiT-T	6	1.1	6682	73.1(+0.9)
DeiT-S [33]	22	4.6	3122	79.8
Random-DeiT-S	22	4.3	3313	80.9(+1.1)
DeiT-B [33]	87	17.6	1226	81.8
Random-DeiT-B	87	17.0	1348	82.5(+0.7)
Partition-Based Backbone				
Swin-T [24]	28	4.5	1738	81.3
Random-Swin-T	28	4.5	1866	82.7(+1.4)
Swin-S [24]	50	8.7	1186	83.0
Random-Swin-S	50	8.7	1248	83.9(+0.9)
Swin-B [24]	88	15.4	864	83.5
Random-Swin-B	88	15.4	902	84.4(+0.9)
CSwin-T [8]	22	4.3	1621	82.7
Random-CSwin-T	22	4.3	1763	83.1(+0.4)
CSwin-S [8]	35	6.9	1036	83.6
Random-CSwin-S	35	6.9	1118	84.2(+0.6)
CSwin-B [8]	78	15.0	716	84.2
Random-CSwin-B	78	15.0	778	84.7(+0.5)
Quadtree-b2 [32]	24	4.5	467	82.7
Random-Quadtree-b2	21	4.3	1926	83.4(+0.7)
Quadtree-b3 [32]	46	7.8	298	83.7
Random-Quadtree-b3	36	7.3	1204	84.3(+0.6)
Quadtree-b4 [32]	64	11.5	188	84.0
Random-Quadtree-b4	49	10.7	703	84.5(+0.5)
BiFormer-T [50]	13	2.2	1704	81.4
Random-BiFormer-T	13	2.2	1903	82.1(+0.7)
BiFormer-STL [50]	28	4.6	1366	82.7
Random-BiFormer-STL	28	4.5	1562	83.1(+0.4)
BiFormer-S [50]	26	4.5	816	83.8
Random-BiFormer-S	26	4.4	1028	84.0(+0.2)
BiFormer-B [50]	57	9.8	544	84.3
Random-BiFormer-B	57	9.6	667	85.1(+0.8)
Pooling-Based Backbone				
PVTv2-B1 [37]	13	2.1	2908	78.7
Random-PVTv2-B1	12	2.2	2898	79.6(+0.9)
PVTv2-B2 [37]	25	4.0	1663	82.0
Random-PVTv2-B2	21	4.2	1678	82.7(+0.7)
PVTv2-B3 [37]	45	6.9	1152	83.2
Random-PVTv2-B3	36	7.2	1187	83.6(+0.4)
Focal-T [45]	29	4.9	583	82.2
Random-Focal-T	28	4.5	1842	82.6(+0.4)
Focal-S [45]	51	9.1	362	83.5
Random-Focal-S	50	8.7	1226	84.2(+0.7)
Focal-B [45]	90	16.0	248	83.8
Ransom-Focal-B	88	15.5	887	84.5(+0.7)

Table 1. Comparison of random grouping strategy with various baselines. The random grouping strategy not only delivers strong performance but also offers faster inference speed compared to other baselines.

Backbone	Params FLOPs		Mask R-CNN 1×						Params FLOPs		RetinaNet 1×					
	(M)	(G)	AP^b	AP_{50}^b	AP_{75}^b	AP^m	AP_{50}^m	AP_{75}^m	(M)	(G)	AP^b	AP_{50}^b	AP_{75}^b	AP_S^b	AP_M^b	AP_L^b
Partition-Based Backbone																
Swin-T [24]	48	267	43.7	66.6	47.7	39.8	63.3	42.7	38	248	41.7	63.1	44.3	27.0	45.3	54.7
Random-Swin-T	48	267	46.0	68.1	50.5	41.9	65.3	45.4	38	248	44.3	65.8	46.9	29.7	47.9	57.8
Swin-S [24]	69	359	45.7	67.9	50.4	41.1	64.9	44.2	60	339	44.5	66.1	47.4	29.8	48.5	59.1
Random-Swin-S	69	359	48.0	69.5	51.9	43.2	67.1	47.0	60	339	46.6	67.8	48.9	30.5	49.3	62.3
Swin-B [24]	107	496	46.9	69.2	51.6	42.3	66.0	45.5	98	477	45.0	66.4	48.3	28.4	49.1	60.6
Random-Swin-B	107	496	49.1	71.6	64.2	44.6	68.2	47.4	98	477	47.4	68.8	50.7	31.3	51.6	64.2
CSwin-T [8]	42	279	46.7	68.6	51.3	42.2	65.6	45.4	–	–	–	–	–	–	–	–
Random-CSwin-T	42	279	47.3	69.3	51.6	42.8	66.4	45.9	–	–	–	–	–	–	–	–
CSwin-S [8]	54	342	47.9	70.1	52.6	43.2	67.1	46.2	–	–	–	–	–	–	–	–
Random-CSwin-S	54	342	48.8	71.3	53.4	44.0	67.9	47.3	–	–	–	–	–	–	–	–
BiFormer-S [50]	45	–	47.8	69.8	52.3	43.2	66.8	46.5	35	–	45.9	66.9	49.4	30.2	49.6	61.7
Random-BiFormer-S	45	265	48.4	70.6	52.4	43.7	67.2	46.9	35	246	46.5	67.4	50.0	30.4	50.6	62.3
Pooling-Based Backbone																
PVTv2-B1 [37]	34	–	41.8	64.3	45.9	38.8	61.2	41.6	24	–	41.2	61.9	43.9	25.4	44.5	54.3
Random-PVTv2-B1	33	216	43.0	66.1	46.9	39.1	52.4	42.9	23	197	42.4	63.0	44.8	26.6	45.2	57.1
PVTv2-B2 [37]	45	–	45.3	67.1	49.6	41.2	64.2	44.4	35	–	44.6	65.6	47.6	27.4	48.8	58.6
Random-PVTv2-B2	41	252	47.1	68.4	51.0	42.4	65.8	45.6	31	233	46.0	66.6	49.2	28.6	50.0	59.9
PVTv2-B3 [37]	65	–	47.0	68.1	51.7	42.5	65.7	45.7	55	–	45.9	66.8	49.3	28.6	49.8	61.4
Random-PVTv2-B3	56	342	47.9	69.3	53.0	43.5	66.2	47.3	46	323	47.0	68.1	49.9	29.8	50.6	62.5

Table 2. Comparison of random grouping strategy with various baselines using RetinaNet and Mask R-CNN on COCO val2017 object detection and instance segmentation.

bone. Specifically, compared to CSwin-S, Random-CSwin-S achieves an increase of +0.9 in AP^b and +0.8 in AP^m . The improvements are even more pronounced when compared to the pooling-based PVTv2.

4.3. Semantic Segmentation

Settings. We adopt the Semantic FPN [19] and UperNet [42] based on MMsegmentation [3] to validate the superiority of random grouping strategy. Following the previous works [12, 18, 30], we train the model for 80k iterations with the framework of Semantic FPN, and train the models for 160k iterations with the framework of UperNet. All models are trained with the input resolution of 512×512 . When testing the model, we resize the shorter side of the image to 512 pixels.

Results. We show the results of semantic segmentation in the Tab. 3. Our simple and fast random grouping method achieves better results compared to various advanced grouping methods. Specifically, under the Semantic FPN framework, using random grouping can achieve a +1.1 mIoU improvement in the base model size compared to the relatively more complex Bi-level routing grouping method in BiFormer.

4.4. Point Cloud Segmentation

Settings. We choose the point cloud segmentation task to further validate the superiority of random grouping. Specifically, we select Point Transformer v3 [40], a powerful point cloud backbone, as our baseline. We train the model on

ScanNet [5] and validate it on the validation set. Latency is tested on an A100 GPU.

Results. As shown in Tab. 4, because our proposed random grouping strategy is simpler and easier to operate compared to the point cloud grouping strategy used in Point Transformer v3, it results in lower inference latency than Point Transformer v3. Additionally, random grouping brings a certain degree of performance improvement to the model.

4.5. Vision Language Models

Settings. We follow the setting of LLaVA-1.5 [22] and LLaVA-1.6 to evaluate the effectiveness of random pattern on the vision-language model. At each Transformer block of the LLM, we permute the input order of vision tokens based on a randomly generated tensor. The positional encodings are aligned with the positions of the vision tokens, while the order of text tokens remains unchanged. The model is trained and evaluated using this strategy.

Results. We show the results in the Tab. 5. Applying random pattern to the vision tokens improve the model’s performance on all benchmarks.

4.6. Why Is Random Grouping Better?

Intuitively, it seems unlikely that a simple random grouping strategy could perform better than other carefully designed, complex methods. Moreover, random grouping causes the model to lose many local biases, making this phenomenon

Model	Semantic FPN 80K			Upernet 160K		
	Params (M)	FLOPs (G)	mIoU (%)	Params (M)	FLOPs (G)	mIoU _{ss} (%)
Plain Backbone						
DeiT-S	-	-	-	52	1099	43.0
Random-DeiT-S	-	-	-	52	1099	44.5
Partition-Based Backbone						
Swin-T [24]	-	-	-	60	945	44.5
Random-Swin-T	-	-	-	60	945	46.8
Swin-S [24]	-	-	-	81	1038	47.6
Random-Swin-S	-	-	-	81	1038	48.9
CSwin-T [8]	26	202	48.2	60	959	49.3
Random-CSwin-T	26	202	48.9	60	959	49.7
CSwin-S [8]	39	271	49.2	65	1027	50.4
Random-Cswin-S	39	271	49.9	65	1027	51.1
CSwin-B [8]	81	464	49.9	109	1222	51.1
Random-Cswin-B	81	464	50.8	109	1222	52.2
BiFormer-S [50]	29	-	48.9	55	-	49.8
Random-BiFormer-S	29	182	49.7	55	935	50.4
BiFormer-B [50]	60	-	49.9	86	-	51.0
Random-BiFormer-B	60	284	51.0	86	1046	52.0
Pooling-Based Backbone						
PVTv2-B1 [37]	18	34	42.5	-	-	-
Random-PVTv2-B1	17	35	43.6	-	-	-
PVTv2-B2 [37]	29	46	45.2	-	-	-
Random-PVTv2-B2	13	48	46.3	-	-	-
PVTv2-B3 [37]	49	62	47.3	-	-	-
Random-PVTv2-B3	40	65	48.8	-	-	-
Focal-T [45]	-	-	-	62	998	45.8
Random-Focal-T	-	-	-	60	945	46.9
Focal-S [45]	-	-	-	85	1130	48.0
Random-Focal-S	-	-	-	81	1038	49.2

Table 3. Comparison of random grouping strategy with various baselines using Semantic FPN and UperNet.

Model	Params (M)	Latency↓ (ms)	mIoU (%)
PTv3 [40]	46	88	77.6
Random-PTv3 [40]	46	68	77.8

Table 4. Comparison of random grouping strategy and baseline on point cloud segmentation.

Model	VQA ^T	MME ^P	GQA	POPE	VQAv2	SEED ^I
LLaVA-1.5	58.2	1511	62.0	86.1	78.5	66.1
+Random Pattern	58.6	1578	62.3	87.4	78.5	66.9
LLaVA-1.6	64.9	1519	64.2	86.5	81.8	70.2
+Random Pattern	65.2	1593	64.5	87.6	82.1	70.6

Table 5. Applying random pattern to LLaVA-1.5/1.6.

even more intriguing. To explain this, we analyze several aspects to understand why such an extremely simple strategy achieves such good results. Our experiments reveal that as long as a few key elements are satisfied, the specific way tokens are grouped becomes less important. Even with an extremely simple method like random grouping, the model

can learn to acquire strong visual representations.

Position Information. When constructing Random-Swin, the token grouping method is completely random, making it impossible to use the original RPE utilized by Swin. Therefore, we replace RPE with CPE [2]. To ensure a fair comparison, we train Swin-T using CPE as the positional encoding. We present the results in Tab. 6. As clearly shown, positional information has a significant impact on random grouping. Unlike window-based grouping, random grouping does not introduce local biases, making positional information particularly crucial. When positional information is added, the performance of the random grouping strategy improves significantly. This indicates that positional information is essential for grouping methods that do not introduce inductive biases.

Model	Params(M)	FLOPs(G)	Acc(%)
Swin-T [24]	28	4.5	81.3
RPE→CPE	28	4.5	81.6
CPE→APE	28	4.5	80.5
CPE→LePE	28	4.5	81.7
w/o PE	28	4.5	80.1(-1.6)
Random-Swin-T	28	4.5	82.7
CPE→APE	28	4.5	82.3
CPE→LePE	28	4.5	83.0
w/o PE	28	4.5	79.3(-3.7)

Table 6. Effect of position information.

To further explore the role of positional information in learning visual features, we qualitatively visualize the attention maps learned by different models. The results are shown in Fig. 4. From the feature maps, it is clear that with positional information, the features learned by Random-Swin are less noisy and more distinct compared to those learned by Swin. However, when positional information is removed, the features learned by both degrade, with Random-Swin experiencing a more severe degradation. Consequently, its performance declines more significantly. This implies that as long as positional information is present, the choice of token grouping strategy becomes less critical.

Head Feature Diversity. For two heads in multi-head attention, m and n , we calculate the cosine similarity between the tokens at all corresponding positions in the two heads, then take the average to obtain the similarity between the feature maps of the two heads. As shown specifically in Eq. 1:

$$\text{Sim}(X_m, X_n) = \frac{\sum_{i=1}^N \cos(X_{mi}, X_{ni})}{N} \quad (1)$$

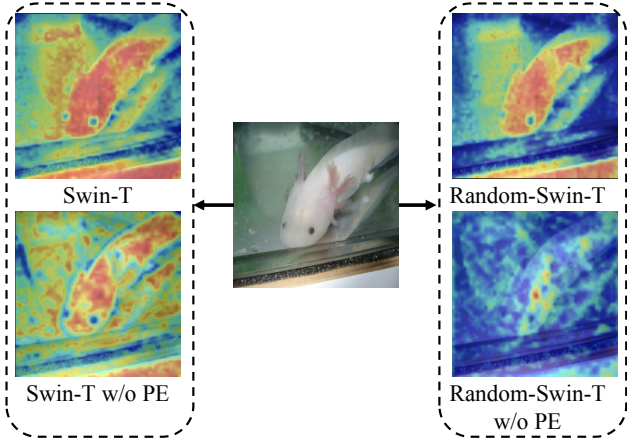


Figure 4. Comparison of attention maps with and without positional information. Positional information is particularly crucial for the random grouping method, which lacks local biases.

where X is the feature map. m, n are the indices of the heads in multi-head attention. i is the index of the token and N is the total number of the token. \cos denotes the cosine similarity. The value of $\text{Sim}(X_m, X_n)$ ranges from 0 to 1, with higher values indicating greater similarity between the two heads.

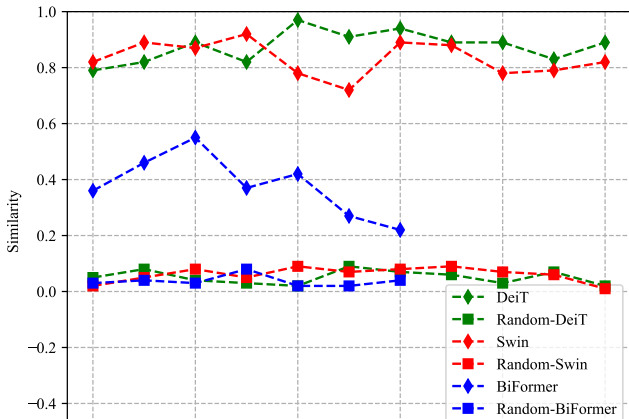


Figure 5. Similarity curves between adjacent heads in different Models

Based on the DeiT-S and the third stage of Swin-T [24], BiFormer-S [50], we visualize the similarity curves between adjacent heads in the feature maps generated by multi-head attention. As shown in Fig. 5, compared to the original model, the models using the random grouping strategy exhibit significantly lower similarity between different heads. This reduction occurs because, in random grouping, each head is associated with a different random tensor, leading to distinct grouping methods for each head and, consequently, significantly different learned features between the heads.

To validate the impact of head feature diversity on model performance, we modify the original random grouping strategy by using a single random tensor P for all heads

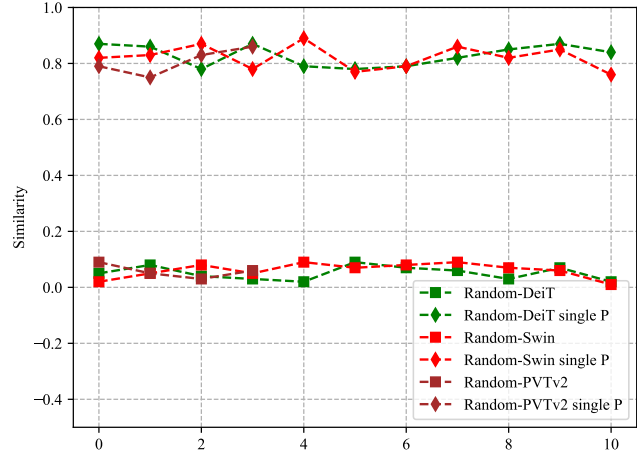


Figure 6. Comparison of each head with a unique random tensor and all heads sharing a single random tensor. Sharing a single random tensor (P) significantly reduces the diversity between different heads.

instead of a different random tensor for each head. This means all heads follow the same random grouping strategy. As shown in Fig. 6, this modification significantly increases the similarity between the heads, indicating a reduction in head feature diversity. As shown in Tab. 7, we provide a

Model	Params(M)	FLOPs(G)	Acc(%)
DeiT-S [33]	22	4.6	79.8
Random-DeiT-S	22	4.3	80.9
multi $P \rightarrow$ single P	22	4.3	79.2(-1.7)
Swin-T [24]	28	4.5	81.3
Random-Swin-T	28	4.5	82.7
multi $P \rightarrow$ single P	28	4.5	80.5(-2.2)
BiFormer-STL [50]	28	4.6	82.7
Random-BiFormer-STL [50]	28	4.5	83.1
multi $P \rightarrow$ single P	28	4.5	80.8(-2.3)
PVTv2-B1 [37]	13	2.1	78.7
Random-PVTv2-B1	12	2.2	79.6
multi $P \rightarrow$ single P	12	2.2	78.1(-1.5)

Table 7. Effect of head feature diversity.

detailed comparison of the impact of head feature diversity on model performance. It is evident that when all heads use the same random strategy, resulting in reduced head feature diversity, the performance of various models significantly declines. This clearly demonstrates the crucial role that head feature diversity plays in learning robust visual features. Additionally, the performance of Random-BiFormer-STL illustrates this point. Since BiFormer-STL inherently has lower feature similarity between heads, indicating greater feature diversity (as shown in Fig. 5), the increase in head feature diversity when using the random grouping strategy is less pronounced, resulting in a smaller performance improvement.

Global Receptive Field. The global receptive field is a significant advantage of Vision Transformers over architectures like CNNs [16, 25]. However, most partition-based methods compromise this by reducing the global receptive field to decrease the model’s computational load [8, 24, 41, 43]. Unlike previous grouping methods, random grouping still manages to sparsely capture global information. This is likely one of the reasons for its superior performance.

To investigate the impact of the global receptive field on model performance, we enhanced the simplest random grouping strategy. Specifically, we constrain the random numbers corresponding to the tokens in each region within certain intervals. Additionally, these intervals for different regions have a certain degree of overlap. This ensures that, during random grouping, most tokens from the same region remain together, while a portion is randomly swapped to other regions.

Model	Params(M)	FLOPs(G)	Acc(%)
DeiT-S [33]	22	4.6	79.8
Random-DeiT-S	22	4.3	80.9
global→region	22	4.3	79.3(-1.6)
Swin-T [24]	28	4.5	81.3
Random-Swin-T	28	4.5	82.7
global→region	28	4.5	81.5(-1.2)
PVTv2-B1 [37]	13	2.1	78.7
Random-PVTv2-B1	12	2.2	79.6
global→region	12	2.2	79.3(-0.3)

Table 8. Effect of global receptive field.

As shown in Tab. 8, we observe that when the global receptive field is sacrificed to a certain degree, the performance of DeiT and Swin drops significantly. This indicates the crucial role that the global receptive field plays in learning visual features. In contrast, the performance drop for PVTv2 is less pronounced. This is because the pooling-based backbone inherently has a global receptive field. The performance decline in PVTv2 may not be due to the loss of the global receptive field but rather because this region-specific random approach reduces the variety of grouping methods for each head in multi-head attention, thereby decreasing head feature diversity.

Fixed Grouping Pattern. Although we use random grouping, the random tensor P that dictates our grouping method is fixed once generated. Therefore, the random grouping remains the same for different input images. In other words, even though it is random grouping, it follows a consistent pattern just like other methods with specific grouping rules.

To verify whether the fixed grouping pattern affects the performance of random grouping, we replace it with a fully random approach. For each input image, we use a

unique random tensor P to determine the random grouping method. This disrupts the fixed grouping pattern in the original random grouping. By doing so, we explore the influence of the fixed grouping pattern on the performance of random grouping. The results, shown in Tab. 9, indicate that when using fully random grouping—where the fixed grouping pattern is disrupted—the performance of all models declines significantly. This clearly demonstrates the crucial role that a fixed grouping pattern plays in the effectiveness of the random grouping strategy.

Model	Params(M)	FLOPs(G)	Acc(%)
DeiT-S [33]	22	4.6	79.8
Random-DeiT-S	22	4.3	80.9
Fully Random	22	4.3	74.3(-6.6)
Swin-T [24]	28	4.5	81.3
Random-Swin-T [24]	28	4.5	82.7
Fully Random	28	4.5	76.4(-6.3)
PVTv2-B1 [37]	13	2.1	78.7
Random-PVTv2-B1	12	2.2	79.6
Fully Random	12	2.2	75.4(-4.2)

Table 9. Effect of the fixed grouping pattern.

Roadmap from Fully Random Grouped Backbone to Random-Swin.

To more clearly illustrate the role of each component, we gradually transform a fully random grouped backbone into Random-Swin-T. By sequentially adding fixed grouping pattern, multi random tensors P , and positional encoding into the backbone, the model’s performance significantly improves. **This validates the conclusion that even very simple random grouping can achieve good results, as long as certain conditions are met.**

Model	Params (M)	FLOPs (G)	Throughput (imgs/s)	Acc (%)
Swin-T	28	4.5	1738	81.3
RPE→CPE	28	4.5	1698	81.6
Fully Random(single P)	28	4.5	1922	71.2
+fixed pattern	28	4.5	1922	77.6
+multi P	28	4.5	1917	80.1
+CPE	28	4.5	1866	82.7

Table 10. Roadmap from fully random grouping backbone to Random-Swin. Inference speed are measured on A100 GPU.

5. Conclusion

In this paper, we pose the question: Are the complex grouping strategies for vision tokens truly necessary? Is there a simpler and more unified token grouping method that can replace these diverse methods? To address these, we propose an extremely simple random grouping strategy. Experiments show that the random grouping strategy outperforms most complex grouping strategies across various

tasks. Moreover, due to its simplicity and ease of implementation, models based on the random grouping strategy achieve faster inference speeds compared to baselines. The success of the random grouping strategy effectively answers our initial questions. To understand the success of this extremely simple grouping strategy, we conduct an in-depth analysis of the underlying factors: positional information, head feature diversity, global receptive field, and a fixed grouping pattern. Our findings demonstrate that as long as these four elements are present, even the simplest random grouping strategy can achieve good results.

References

- [1] Kai Chen, Jiaqi Wang, Jiangmiao Pang, et al. MMDetection: Open mmlab detection toolbox and benchmark. *arXiv preprint arXiv:1906.07155*, 2019. 4
- [2] Xiangxiang Chu, Zhi Tian, Bo Zhang, Xinlong Wang, and Chunhua Shen. Conditional positional encodings for vision transformers. In *ICLR*, 2023. 6
- [3] MMSegmentation Contributors. Mmsegmentation, an open source semantic segmentation toolbox, 2020. 5
- [4] Ekin D Cubuk, Barret Zoph, Jonathon Shlens, et al. Randaugment: Practical automated data augmentation with a reduced search space. In *CVPRW*, 2020. 2, 4
- [5] Angela Dai, Angel X. Chang, Manolis Savva, Maciej Halber, Thomas Funkhouser, and Matthias Nießner. Scannet: Richly-annotated 3d reconstructions of indoor scenes. In *Proc. Computer Vision and Pattern Recognition (CVPR), IEEE*, 2017. 5
- [6] Jia Deng, Wei Dong, Richard Socher, et al. Imagenet: A large-scale hierarchical image database. In *CVPR*, 2009. 4
- [7] Mingyu Ding, Bin Xiao, Noel Codella, et al. Davit: Dual attention vision transformers. In *ECCV*, 2022. 2, 3
- [8] Xiaoyi Dong, Jianmin Bao, Dongdong Chen, et al. Cswin transformer: A general vision transformer backbone with cross-shaped windows. In *CVPR*, 2022. 1, 3, 4, 5, 6, 8
- [9] Alexey Dosovitskiy, Lucas Beyer, Alexander Kolesnikov, et al. An image is worth 16x16 words: Transformers for image recognition at scale. In *ICLR*, 2021. 1, 2
- [10] Qihang Fan, Huaibo Huang, Jiyang Guan, and Ran He. Rethinking local perception in lightweight vision transformer, 2023. 2
- [11] Qihang Fan, Huaibo Huang, Mingrui Chen, and Ran He. Semantic equitable clustering: A simple, fast and effective strategy for vision transformer, 2024. 1, 3
- [12] Qihang Fan, Huaibo Huang, Mingrui Chen, Hongmin Liu, and Ran He. Rmt: Retentive networks meet vision transformers. In *CVPR*, 2024. 2, 5
- [13] SG-Former: Self guided Transformer with Evolving Token Reallocation. Sucheng ren, xingyi yang, songhua liu, xincao wang. In *ICCV*, 2023. 2
- [14] Jianyuan Guo, Kai Han, Han Wu, Chang Xu, Yehui Tang, Chunjing Xu, and Yunhe Wang. Cmt: Convolutional neural networks meet vision transformers. In *CVPR*, 2022. 1, 3
- [15] Ali Hassani, Steven Walton, Jiachen Li, Shen Li, and Humphrey Shi. Neighborhood attention transformer. In *CVPR*, 2023. 3
- [16] Kaiming He, Xiangyu Zhang, Shaoqing Ren, and Sun Jian. Deep residual learning for image recognition. In *CVPR*, 2016. 8
- [17] Kaiming He, Georgia Gkioxari, Piotr Dollár, and Ross B. Girshick. Mask r-cnn. In *ICCV*, 2017. 4
- [18] Huaibo Huang, Xiaoqiang Zhou, and Ran He. Orthogonal transformer: An efficient vision transformer backbone with token orthogonalization. In *NeurIPS*, 2022. 5
- [19] Alexander Kirillov, Ross Girshick, Kaiming He, and Piotr Dollár. Panoptic feature pyramid networks. In *CVPR*, 2019. 5
- [20] Youwei Liang, Chongjian Ge, Zhan Tong, Yibing Song, Jue Wang, and Pengtao Xie. Not all patches are what you need: Expediting vision transformers via token reorganizations. In *International Conference on Learning Representations*, 2022. 2
- [21] Tsung-Yi Lin, Priya Goyal, Ross B. Girshick, and Kaiming He and Piotr Dollár. Focal loss for dense object detection. In *ICCV*, 2017. 4
- [22] Haotian Liu, Chunyuan Li, Yuheng Li, and Yong Jae Lee. Improved baselines with visual instruction tuning, 2023. 4, 5
- [23] Kai Liu, Tianyi Wu, Cong Liu, and Guodong Guo. Dynamic group transformer: A general vision transformer backbone with dynamic group attention. In *IJCAI*, 2022. 2, 3
- [24] Ze Liu, Yutong Lin, Yue Cao, Han Hu, Yixuan Wei, Zheng Zhang, Stephen Lin, and Baining Guo. Swin transformer: Hierarchical vision transformer using shifted windows. In *ICCV*, 2021. 1, 2, 3, 4, 5, 6, 7, 8
- [25] Zhuang Liu, Hanzi Mao, Chao-Yuan Wu, et al. A convnet for the 2020s. In *CVPR*, 2022. 8
- [26] Junting Pan, Adrian Bulat, Fuwen Tan, et al. Edgevits: Competing light-weight cnns on mobile devices with vision transformers. In *ECCV*, 2022. 2
- [27] Zizheng Pan, Jianfei Cai, and Bohan Zhuang. Fast vision transformers with hilo attention. In *NeurIPS*, 2022. 3
- [28] Boris T Polyak and Anatoli B Juditsky. Acceleration of stochastic approximation by averaging. *arXiv preprint arXiv:1906.07155*, 2019. 2
- [29] Yongming Rao, Wenliang Zhao, Benlin Liu, Jiwen Lu, Jie Zhou, and Cho-Jui Hsieh. Dynamicvit: Efficient vision transformers with dynamic token sparsification. In *NeurIPS*, 2021. 2
- [30] Yongming Rao, Wenliang Zhao, Yansong Tang, Jie Zhou, Ser-Lam Lim, and Jiwen Lu. Hornet: Efficient high-order spatial interactions with recursive gated convolutions. In *NeurIPS*, 2022. 5
- [31] Chenyang Si, Weihao Yu, Pan Zhou, Yichen Zhou, Xinchao Wang, and Shuicheng YAN. Inception transformer. In *NeurIPS*, 2022. 2
- [32] Shitao Tang, Jiahui Zhang, Siyu Zhu, et al. Quadtree attention for vision transformers. In *ICLR*, 2022. 1, 2, 3, 4
- [33] Hugo Touvron, Matthieu Cord, Matthijs Douze, et al. Training data-efficient image transformers & distillation through attention. In *ICML*, 2021. 2, 4, 7, 8

- [34] Hugo Touvron, Matthieu Cord, Alexandre Sablayrolles, Gabriel Synnaeve, and Hervé Jégou. Going deeper with image transformers. In *ICCV*, 2021. [2](#)
- [35] Ashish Vaswani, Noam Shazeer, Niki Parmar, et al. Attention is all you need. In *NeurIPS*, 2017. [1](#), [2](#)
- [36] Wenhai Wang, Enze Xie, Xiang Li, Deng-Ping Fan, Kaitao Song, Ding Liang, Tong Lu, Ping Luo, and Ling Shao. Pyramid vision transformer: A versatile backbone for dense prediction without convolutions. In *ICCV*, 2021. [1](#), [2](#), [4](#)
- [37] Wenhai Wang, Enze Xie, Xiang Li, Deng-Ping Fan, Kaitao Song, Ding Liang, Tong Lu, Ping Luo, and Ling Shao. Pvtv2: Improved baselines with pyramid vision transformer. *Computational Visual Media*, 8(3):1–10, 2022. [1](#), [3](#), [4](#), [5](#), [6](#), [7](#), [8](#)
- [38] Wenxiao Wang, Lu Yao, Long Chen, Binbin Lin, Deng Cai, Xiaofei He, and Wei Liu. Crossformer: A versatile vision transformer hinging on cross-scale attention. In *ICLR*, 2022. [1](#), [2](#)
- [39] Yulin Wang, Rui Huang, Shiji Song, Zeyi Huang, and Gao Huang. Not all images are worth 16x16 words: Dynamic vision transformers with adaptive sequence length. In *NeurIPS*, 2021. [2](#)
- [40] Xiaoyang Wu, Li Jiang, Peng-Shuai Wang, Zhijian Liu, Xihui Liu, Yu Qiao, Wanli Ouyang, Tong He, and Hengshuang Zhao. Point transformer v3: Simpler, faster, stronger. In *CVPR*, 2024. [4](#), [5](#), [6](#)
- [41] Zhuofan Xia, Xuran Pan, Shiji Song, Li Erran Li, and Gao Huang. Vision transformer with deformable attention. In *CVPR*, 2022. [1](#), [3](#), [8](#)
- [42] Tete Xiao, Yingcheng Liu, Bolei Zhou, Yuning Jiang, and Jian Sun. Unified perceptual parsing for scene understanding. In *ECCV*, 2018. [5](#)
- [43] Chenglin Yang, Yilin Wang, Jianming Zhang, et al. Lite vision transformer with enhanced self-attention. In *CVPR*, 2022. [8](#)
- [44] Chenglin Yang, Siyuan Qiao, Qihang Yu, et al. Moat: Alternating mobile convolution and attention brings strong vision models. In *ICLR*, 2023. [2](#)
- [45] Jianwei Yang, Chunyuan Li, Pengchuan Zhang, Xiyang Dai, Bin Xiao, Lu Yuan, and Jianfeng Gao. Focal self-attention for local-global interactions in vision transformers. In *NeurIPS*, 2021. [2](#), [4](#), [6](#)
- [46] Ting Yao, Yehao Li, Yingwei Pan, Yu Wang, Xiao-Ping Zhang, and Tao Mei. Dual vision transformer. *TPAMI*, 2023. [2](#)
- [47] Sangdoon Yun, Dongyoon Han, Seong Joon Oh, et al. Cutmix: Regularization strategy to train strong classifiers with localizable features. In *ICCV*, 2019. [4](#)
- [48] Hongyi Zhang, Moustapha Cisse, Yann N Dauphin, et al. mixup: Beyond empirical risk minimization. In *ICLR*, 2018. [4](#)
- [49] Zhun Zhong, Liang Zheng, Guoliang Kang, et al. Random erasing data augmentation. In *AAAI*, 2020. [2](#), [4](#)
- [50] Lei Zhu, Xinjiang Wang, Zhanghan Ke, Wayne Zhang, and Rynson Lau. Biformer: Vision transformer with bi-level routing attention. In *CVPR*, 2023. [1](#), [2](#), [3](#), [4](#), [5](#), [6](#), [7](#)